Applied Catalysis B: Environmental 123–124 (2012) 151–161

Contents lists available at SciVerse ScienceDirect

Applied Catalysis B: Environmental

journal homepage: www.elsevier.com/locate/apcatb

Photo-assisted degradation of 2,4,5-trichlorophenoxyacetic acid by Fe(II)-catalyzed activation of Oxone process: The role of UV irradiation, reaction mechanism and mineralization

Y.R. Wang, W. Chu*

Department of Civil and Structural Engineering, Research Centre for Urban Environmental Technology and Management, The Hong Kong Polytechnic University, Hung Hom, Kowloon, Hong Kong

ARTICLE INFO

Article history:
Received 5 February 2012
Received in revised form 14 April 2012
Accepted 22 April 2012
Available online 26 April 2012

Keywords:
2,4,5-Trichlorophenoxyacetic acid
Oxone
Hydroxyl radical
Sulfate radical
UV irradiation

ABSTRACT

In this study, the potential of Fe(II)-catalyzed activation of Oxone process with UV irradiation (FOU) for the degradation of 2,4,5-trichlorophenoxyacetic acid (2,4,5-T) in aqueous solution was explored and compared with the Fe(II)/Oxone (FO) process. Experimental results show that the FO process was dramatically promoted upon the introduction of UV irradiation. As a result, the role of UV irradiation was elucidated in-depth by comparing the real-time of [Fe(II)] between the FO process and the FOU process. It was found that a beneficial Fe(III)/Fe(II) catalytic cycle is established in the presence of UV irradiation, thereby leading to the accelerated regeneration of Fe(II). Additionally, 2,4,5-T decay by the FOU process under various [Oxone] and [2,4,5-T] was also examined. Furthermore, the decay pathways for the transformation of 2,4,5-T by UV alone, Oxone/UV, and FOU processes were proposed by using LC-ESI/MS analysis. Distinct differences of intermediate distributions were observed among the three processes with or without the involvement of radicals ($^{\bullet}OH$ and $SO_4^{\bullet-}$). Besides, the efficiencies of various processes (i.e., UV alone, Oxone/UV and FOU) were further examined in terms of mineralization and Cl^- ion accumulation.

1. Introduction

Oxone®, the commercial name of a triple potassium salt ($2KHSO_5{\cdot}KHSO_4{\cdot}K_2SO_4$), is the source of active ingredient potassium peroxymonosulfate, HSO_5^-, which has a higher potential than that of H_2O_2 ($E^0_{HSO_5^-/HSO_4^-} = +1.82\,V$; $E^0_{H_2O_2/H_2O} = +1.776\,V$) [1]. Compared to H_2O_2, Oxone is relatively stable at room temperature and easy of handling due to its solid state. Consequently, Oxone has attracted increasing attention in the field of wastewater treatment [2–4]. However, direct reactions of Oxone with organics are generally slow at room temperature, whereas Oxone can be easily activated into highly reactive radicals ($SO_4^{\bullet-}$ and $^{\bullet}OH$) through homolytic cleavage of the peroxide bond of HSO_5^- by photolysis or thermolysis (Eq. (1)) or into $SO_4^{\bullet-}$ via one electron transfer (Eq. (2)) by transition metal (e.g. Co^{2+} and Fe^{2+}):

$$HSO_5^- \xrightarrow{h\nu/\Delta} SO_4^{\bullet-} + {}^{\bullet}OH \quad (1)$$

$$HSO_5^- + M^{n+} \rightarrow SO_4^{\bullet-} + M^{(n+1)+} + OH^- \quad (2)$$

Recently, Oxone activated by transition metals has been extensively investigated to treat various organic compounds in the aqueous solution [5,6]. One of the most commonly used combinations is the coupling of Fe(II) with Oxone. However, similar to the Fenton process, the slow regeneration of Fe(II) and production of ferric hydroxide sludge restrict its usage. One way to improve the above process is the application of UV irradiation, which may potentially improve the reaction through:

(1) The use of UV (≤260 nm) irradiation promotes the production of both $SO_4^{\bullet-}$ and $^{\bullet}OH$ through Eq. (1) [4,7].
(2) In the presence of UV irradiation, the Fe(III)/Fe(II) catalytic cycle is accelerated by the photo-reduction of Fe(III)-complexes, in which Fe^{3+} can exist as ferric ions and/or Fe(III)-complexes (such as $[Fe(H_2O)_6]^{3+}$, $[Fe(OH)]^{2+}$, $[Fe(OH)_2]^+$ and $[Fe_2(OH)_2]^{4+}$) depending on the solution pH [8]. For example, $Fe(OH)^{2+}$, as the principal species at pH range of 2.5–4.0 [9], is photosensitive according to Eq. (3) [10]:

$$Fe(OH)^{2+} + h\nu \rightarrow Fe^{2+} + {}^{\bullet}OH \quad (3)$$

It should be noted that the above reaction can not only accelerate the regeneration of ferrous ions but also produce additional hydroxyl radicals.

Obviously, the dominant oxidants in the FOU process are hydroxyl and sulfate radicals. They react with organics mainly through the mechanisms of electron transfer, H-abstraction, and

* Corresponding author. Tel.: +852 2766 6075; fax: +852 2334 6389.
E-mail address: cewchu@polyu.edu.hk (W. Chu).

0926-3373/$ – see front matter © 2012 Elsevier B.V. All rights reserved.
http://dx.doi.org/10.1016/j.apcatb.2012.04.031

hydrogen addition [11]. Generally, $SO_4^{\bullet-}$ reacts more selectively with target compounds through electron transfer, while •OH induces reactions more readily via H-abstraction or addition [12]. Nevertheless, the majority of the products formed by sulfate radical attack on aromatics are hydroxylation products, which are in accordance with the intermediates from hydroxyl radical attack [13].

The compound 2,4,5-T is extensively used in many countries for weed control [14]. It is considered to be less readily biodegradable than the analogous phenoxyacetic acid herbicides (e.g. 2,4-dichlorophenoxyacetic acid, 2,4-D) due to the additional chlorine on the aromatic ring [15]. It has potential toxicity toward humans and animals. Human exposure to 2,4,5-T has been associated with numerous clinical manifestations, such as nervous system and brain damage. Additionally, this compound may be contaminated by dioxins during the production process, which imposes the potential of high toxicity to the environment [16]. As a result, the degradation of 2,4,5-T has been investigated by using various treatment processes, such as the electrochemical method [17], peroxi-coagulation [18], electro-Fenton method [19], photoelectron-Fenton process [20], and TiO_2 mediated photocatalysis [21]. Though, some simple degradation intermediates resulting from those degradation processes have been demonstrated, a systematically study on the 2,4,5-T decay mechanisms by the FOU process is very limited.

Against the above background, FOU process is proposed as a possible alternative for the wastewater treatment in this study. An attempt was made to elucidate the role of UV irradiation in FOU process as compared to the conventional FO process. Another objective of this study is to identify the aromatic intermediates formed during the decay of 2,4,5-T by the proposed FOU (via $SO_4^{\bullet-}$ and •OH attack) through the examination and comparison of the probe decay by UV alone and Oxone/UV processes. Special attention has been paid to analyzing the reaction mechanisms that rule the process. Furthermore, the mineralization and the release of chloride ions by these three processes have also been studied.

2. Experimental

2.1. Chemicals and reagents

All chemicals are of analytic reagent grade and all solvents are of HPLC grade; they were used as received without further purification. The 2,4,5-T ($C_8H_5Cl_3O_3$, 97%), Oxone (95%), $FeSO_4{\cdot}7H_2O$ (99.0%) were purchased from Sigma–Aldrich Inc. (USA), while 1,10-phenanthroline was purchased from International Laboratory (IL, USA). The 2,4,5-trichlorophenol (2,4,5-TCP) and 2,4-dichlorophenol (2,4-DCP, neat) were obtained from Wako Pure Chemical Industries Ltd. and Supelco, respectively. The salts supplying anions used in this study including Na_2CO_3, $NaHCO_3$, NaH_2PO_4, CH_3COONa and $Na_2C_2O_4$ were obtained from British Drug Houses (BDH, England). Distilled-deionized water with a resistivity of 18.2 MΩ cm generated from a Bamstead NANOpure water treatment system (Thermo Fisher Scientific Inc., USA) was used to prepare all the solutions. Acetonitrile (Tedia Company Inc.) was degassed before being used in high performance liquid chromatography (HPLC). Nitric acid and/or sodium hydroxide were used to adjust the initial pH of the solutions.

2.2. Experimental procedures

All the experiments were performed in an air-conditioned laboratory at 23 ± 2 °C. The FOU reactions were conducted in a 50 mL quartz beaker placed in the center of a CCP-4V photochemical reactor purchased from Luzchem Research Inc. [22]. A cooling fan was installed in the photochemical reactor to control the temperature. Two phosphor-coated low-pressure mercury lamps emitting monochromatic light at 254 nm with light intensity of 1.5×10^{-6} Einstein L^{-1} s^{-1} for each lamp were symmetrically arranged within the photoreactor as the irradiation source. For the wavelength effect tests, four different lamps at 254, 300, 350 and 419 nm were investigated. Each of the latter three types of UV lamp generates a light intensity of around 10^{-6} Einstein L^{-1} s^{-1} determined by ferrioxalate actinometry [23]. The Fe(II) and Oxone solutions were freshly prepared before each test. For each test, a proper amount of Fe^{2+} catalyst was added to the aqueous solution containing the probe contaminant. Then, the reaction was initiated by the addition of an appropriate amount of Oxone and simultaneously switching on the UV lamps. If the lamps are cool, they need to be warmed up for 10 min in advance to ensure a stable light source. The initial volume of the solution was fixed at 50 mL. The solution was stirred by a magnetic bar to maintain complete homogeneity throughout the reaction. Samples of 0.5 mL were withdrawn from the photoreactor at specific time intervals and immediately mixed with the same amount of methanol to quench the reaction. The FO tests were conducted in the same quartz beaker and the same procedures were followed without using irradiation. In terms of TOC measurement, sodium azide was used as the quenching agent to minimize any interference. All the tests were duplicated and average values were used in presenting the results. It should be noted that the addition of 0.25 mM Oxone resulted in a solution pH of ~3.68 if no pH adjustment, and this pH level was used throughout this study, unless stated otherwise.

2.3. Analytical methods

The residual 2,4,5-T was quantified by HPLC which consists of a Waters 515 HPLC pump, a Waters 717 plus Autosampler, a C18 reversed phase column (250 mm × 4.6 mm with i.d. of 5 μm, Restek), and a Waters 2489 UV/vis detector. The mobile phase was a mixture of acetonitrile and water in a ratio of 50:50 and then was added 0.05% (v/v) phosphoric acid. The elution flow rate was adjusted to 1.2 mL min^{-1} and the injection volume was 10 μL. The UV/vis detector wavelength was set at 289 nm, which is the maximum absorbance wavelength of 2,4,5-T determined by scanning its spectra from 200 to 900 nm using a spectrophotometer Spectronic (R) Genesys™.

The identification of aromatic intermediates was conducted by a Finnigan SpectraSYSTEM® LC cooperated with a Thermo Quest Finnigan LCQ Duo mass spectrometer system which was equipped with an electrospray ionization interface operating at a negative mode (LC-ESI/MS). The effluent (1.0 mL min^{-1}) was delivered by a gradient system from a Thermo P4000 partitioned by the same column described before. The mobile phase was a mixture of 0.05% acetic acid (A) and 100% acetonitrile (B), which was carried out with a gradient mode according to the following: (1) 100% of A was kept during the first 2 min; (2) from 2 to 47 min, B was linearly increased from 0 to 60%, while A was steadily decreased to 40%, where held for 5 min; and (3) from 52 to 55 min, the mobile phase was turned to the initial composition until the end of the run. If the intermediate compounds cannot commercially be purchased, they were quantified by comparing their ion intensities with that of the probe compound. This approximation is acceptable based on the fact that the UV absorbance may be ascribed to the resonance structure of the ring, which is basically identical [24].

The quantification of Fe(II) (in both ionic and complex forms) was monitored by spectrophotometric method at 510 nm after adding 1,10-phenanthroline to form the reddish Fe(II)–phenanthroline complexes. The detection limit of this method for Fe(II) was 1.8×10^{-4} mM [25]. TOC was measured by a Shimadzu TOC-5000A analyzer equipped with an ASI-5000A

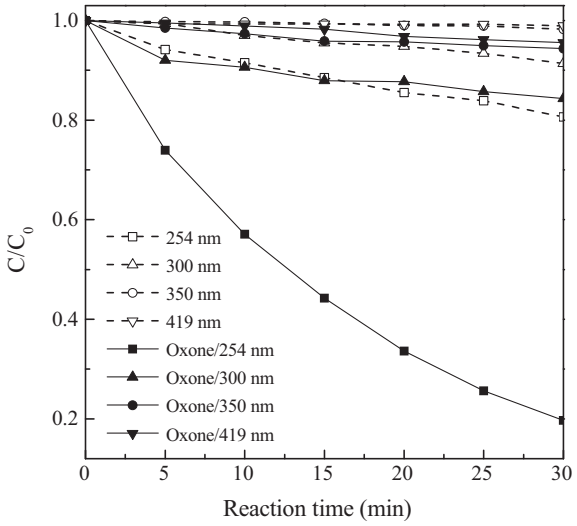

Fig. 1. Comparison of 2,4,5-T degradation by direct photolysis and Oxone/UV. *Experimental conditions*: $[2,4,5\text{-T}]_0 = 0.1$ mM, $[\text{Oxone}]_0 = 0.25$ mM, two UV lamps were employed.

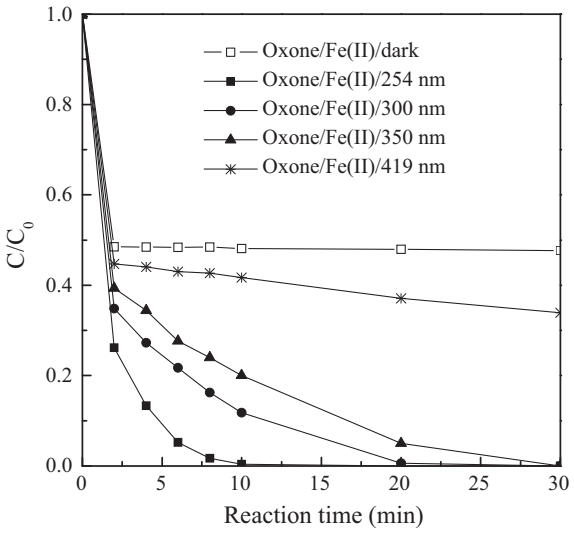

Fig. 2. 2,4,5-T photodegradation by FOU process under different wavelengths. *Experimental conditions*: $[2,4,5\text{-T}]_0 = 0.1$ mM, $[\text{Oxone}]_0 = [\text{Fe(II)}]_0 = 0.25$ mM, two UV lamps were employed.

autosampler. The concentration of Cl^- was determined by ion chromatography (Dionex Series 4500i) equipped with a Dionex IonPac® AS14 anion column (4 mm × 250 mm), using a mixture of 1 mM $NaHCO_3$ and 3.5 mM Na_2CO_3 at 1 mL min^{-1} as mobile phase.

3. Results and discussion

3.1. Comparison of direct photolysis and Oxone/UV

Preliminary tests were conducted to investigate the contributions of direct photolysis (UV or near Visible) and UV-assisted activation of Oxone (Oxone/UV or near Visible) to the photodegradation of 2,4,5-T in aqueous solution. As shown in Fig. 1, the direct photolysis of 2,4,5-T under visible light (419 nm) or near-UV radiation (350 nm) is negligible (<2%), and slow direct photolysis was observed at 9% and 19% in 30 min for UV 300 and UV 254 nm, respectively. The combination of Oxone and UV irradiation enhanced the efficiency of probe decay compared to that of direct photolysis. However, inappreciable promotion (<7%) of 2,4,5-T degradation was obtained when the wavelength is above 300 nm, suggesting the introduction of UV-A or visible irradiation cannot effectively activate the decomposition of Oxone. In contrast, over 80% removal of 2,4,5-T was achieved by Oxone/UV-C process in 30 min. This significant improvement under UV 254 nm irradiation is apparently attributed to the photolysis of Oxone as indicated in Eq. (1). Stoichiometrically, the photolysis of 1 mole HSO_5^- leads to the generation of 1 mole $^{\bullet}OH$ and 1 mole $SO_4^{\bullet -}$ via the homolytic cleavage of its asymmetrical structure. Thus, radical-based oxidation mechanism in Oxone/UV-C process plays a critical role in the degradation of the probe. Additionally, the decay of 2,4,5-T by Oxone/UV-C was found to follow pseudo first-order kinetics with a rate constant of 5.45×10^{-2} min^{-1}, which is around 6.26 times higher than that of UV alone at 254 nm. The differences in photo-assisted activation of Oxone at various wavelengths can be rationalized from the following reasons. First, it was reported that little or no photochemical decomposition of Oxone is observed if the wavelength is higher than 260 nm [4]. Secondly, the adsorption coefficient of a particular species is a key factor determining the adsorption behavior under UV irradiation. According to Anipsitakis and Dionysiou [26], the molar extinction coefficient of Oxone sharply decreases as wavelength increases from 190 to 260 nm. Thus, UV 254 nm stands out for the decomposition of Oxone in this study.

3.2. Fe(II)-activated Oxone under irradiation at various wavelengths

Fig. 2 shows the process performance by FO under irradiation at various wavelengths. For comparison purpose, 2,4,5-T degradation in FO without UV irradiation was also examined. From Fig. 2, the overall removal efficiency was 53% for the FO/dark process; and this conventional FO process showed a rapid 2,4,5-T decay in the first few minutes, followed by a retarded second stage, where no appreciable degradation took place. The reaction mechanism of FO process was well elucidated in our previous study [27], where the fast reactive-stage was attributed to the immediate generation of sulfate radicals upon the mixing of Fe(II) and Oxone. The lag stage was due to the slow regeneration of Fe(II) from Fe(III), in which the Fe(III)/Fe(II) recycling is considered as the rate-limiting step for the conventional FO process. However, when UV irradiation is involved, the performance is obviously enhanced due to the synergistic effects as mentioned in the introduction of the present paper. In addition, the introduction of photo irradiation leads to a 100% 2,4,5-T removal at 254, 300 and 350 nm in 10, 20 and 30 min, respectively. The enhancement was insignificant when 419 nm was employed, which is due to a much lower light absorption of Fe(III)-complexes at 419 nm [9,28]. As a result, considering the performance of UV-C in activating the photolysis of Oxone and facilitating the regeneration Fe(III)/Fe(II) catalysts, the wavelength of 254 nm was chosen exclusively as the light source for the rest of this study.

3.3. Effect of [Fe(II)] and the role of UV irradiation

To examine the effect of [Fe(II)] and better understand the role of UV irradiation, two sets of experiments were conducted: (1) 2,4,5-T degradation by the FO process under various [Fe(II)] from 0.002 to 5.0 mM; and (2) applying UV-C at 254 nm to the process while keeping other parameters constant. Figs. 3 and 4 show the degradation of 2,4,5-T under various [Fe(II)] and the corresponding change in the remaining [Fe(II)] during the reaction by the FO and FOU, respectively. It should be pointed out that the evolution profile of Fe(II) at 0.002 mM was not given due to the limitation of detection. For the FO process, the addition of ferrous ions may either enhance or inhibit the degradation efficiency depending on the [Fe(II)], as shown in Fig. 3a. Generally, the 2,4,5-T degradation

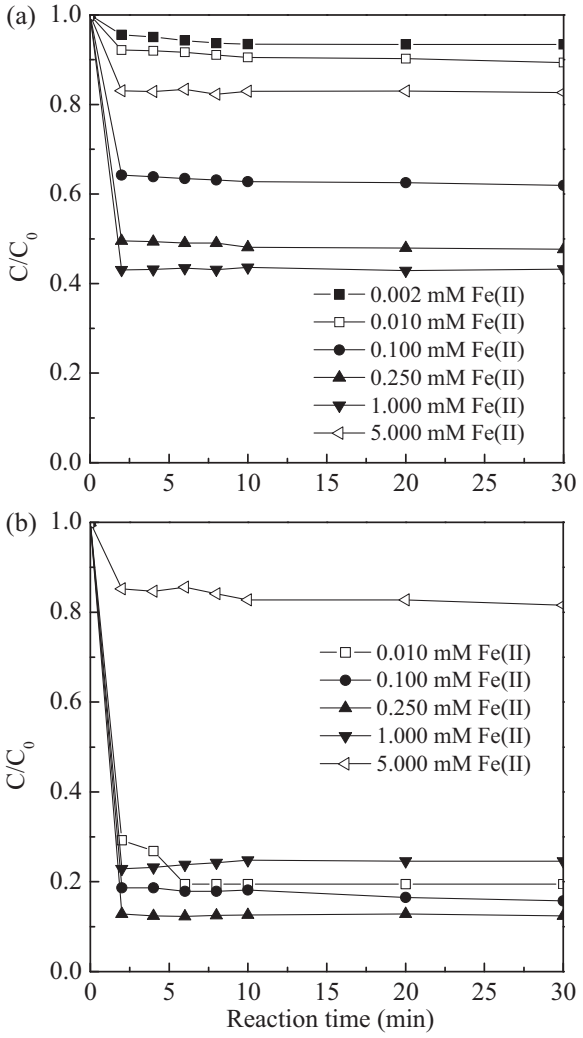

Fig. 3. (a) Effect of Fe(II) dosage on the photodegradation of 2,4,5-T by FO system. (b) Change of the remaining [Fe(II)] over reaction time. *Experimental conditions*: $[2,4,5\text{-T}]_0 = 0.1$ mM, $[\text{Oxone}]_0 = 0.25$ mM.

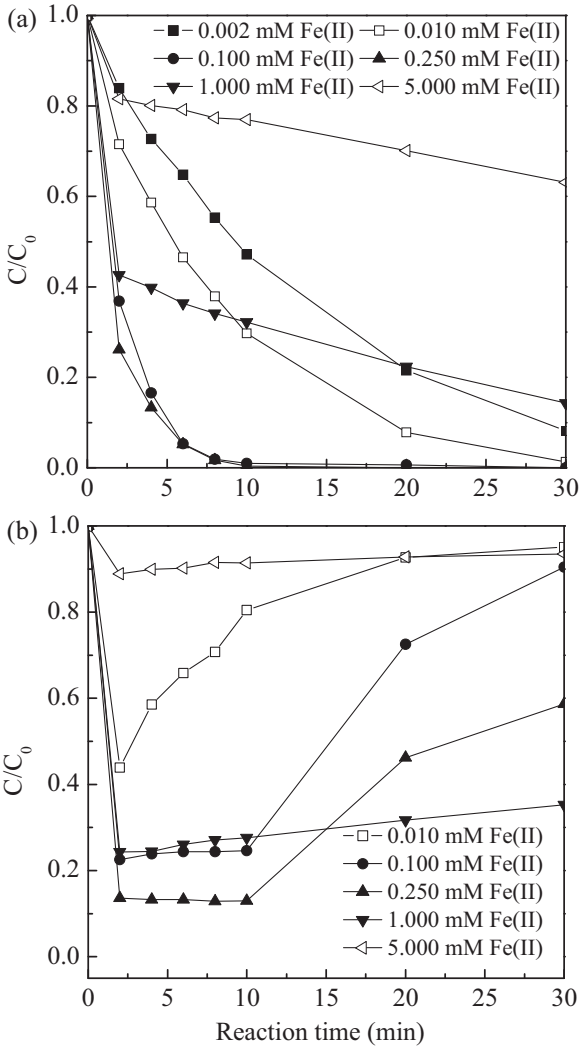

Fig. 4. (a) Effect of Fe(II) dosage on the photodegradation of 2,4,5-T by FOU process. (b) Change in the remaining [Fe(II)] over reaction time. *Experimental conditions*: $[2,4,5\text{-T}]_0 = 0.1$ mM, $[\text{Oxone}]_0 = 0.25$ mM, two 254 nm UV lamps were employed.

efficiency firstly increases from 6.6% to 56.8% as [Fe(II)] increases from 0.002 to 1.0 mM (corresponding to a Fe(II)/Oxone ratio of 0.008–4.0) and then significantly decreases to 17.3% as [Fe(II)] further increases to 5.0 mM (Fe(II)/Oxone = 20). An optimal [Fe(II)] was therefore observed for the FO process. This phenomenon is similar to the Fenton process with an optimal catalyst dose of iron. Previous studies [6,27] also reported that optimal molar ratio of Fe(II)/Oxone at 1:1 or 2:1 (stoichiometric) was observed in FO process, suggesting that ferrous ions do not demonstrate true catalytic activity in FO process. Thus, an optimal [Fe(II)] in this study was found around 1.0 mM, which corresponds to a Fe(II)/Oxone ratio of 4.

When the [Fe(II)] is low in the solution, the lower probe degradation efficiency results from the slower Fe(II) regeneration (i.e., the rate-limiting step) [27]. To verify this, the [Fe(II)] was monitored as shown in Fig. 3b, where the rapid reaction of Oxone with ferrous ions leads to a fast consumption (>80%) of [Fe(II)] in the first few minutes (a similar trend of 2,4,5-T decay was observed simultaneously, see Fig. 3a), and no regeneration of [Fe(II)] was observed throughout the test. On the other hand, the addition of excessive ferrous ions will retard the process due to the $SO_4^{\bullet-}$-scavenging effect by overdosed Fe(II) as shown in Eq. (4):

$$Fe^{2+} + SO_4^{\bullet-} \rightarrow Fe^{3+} + SO_4^{2-} \quad (4)$$

For the overdosed case using 5.0 mM Fe(II) (Fig. 3b), over 81% of ferrous ions remained unreacted in the solution, while only 18% of 2,4,5-T was decayed as one of the worst cases. This is, unlikely due to the underdose of Oxone (since the cases of lower [Fe(II)] have shown better performance), but more precisely attributed to the futile consumption of precious radicals by non-target components in the solution such as the ferrous ions in Eq. (4). This observation therefore provides a strong evidence to justify the quenching of sulfate radicals by high dose of ferrous ions.

In the presence of the UV irradiation, however the trends of 2,4,5-T degradation and [Fe(II)] profiles changed dramatically. As illustrated in Fig. 4a, the photo-decay of 2,4,5-T was significantly improved under various [Fe(II)] by the FOU process. It is believed that a beneficial Fe(III)/Fe(II) cycle has been established due to the introduction of UV irradiation simply by comparing Figs. 3b and 4b. In general, for the investigated [Fe(II)] range of 0.002–5.0 mM, two distinct types of 2,4,5-T degradation tendencies were observed.

Type one: the probe degradation increases with the increment of ferrous dosage and follows pseudo first-order kinetics with the ascending rate constant of 0.76×10^{-1}, 1.26×10^{-1}, 4.86×10^{-1} and 5.08×10^{-1} min^{-1} for 0.002, 0.01, 0.1 and 0.25 mM Fe(II), respectively. The quickest 2,4,5-T decay is observed around 0.1–0.25 mM Fe(II), in which 2,4,5-T was completely removed in 10 min for

both cases. Their corresponding [Fe(II)] trends (see Fig. 4b) rapidly dropped in the first 2 min, then leveled off in the following 8 min and significantly increased afterward. The fast reaction upon the interaction of Fe(II) and Oxone is responsible for the sudden [Fe(II)] drop within the first 2 min; the following steady stage in Fe(II) concentration is likely a steady state between the consumption and regeneration of Fe(II). The [Fe(II)] increment at final stage is likely due to the consumption of Fe(II) being terminated after the total exhaustion of Oxone, while the regeneration of Fe(II) via the photolysis of Fe(III) remaining.

Type two: upon the further increase of [Fe(II)] over 0.25 mM, the photodegradation of the probe was hindered with the increment of ferrous dosage. Under these circumstances, as shown in Fig. 4a, the probe decay was divided into a two-step kinetics: a rapid initial decay (during the initial 2 min) followed by a slower retardation stage. Concurrently, the [Fe(II)] shows a sudden drop in the first two min and then gradually increases as shown in Fig. 4b. For the initial rapid decay stage, there is no significant difference between the FO and FOU by comparing Figs. 3a and 4a. However, the presence of UV irradiation apparently exhibits its advantage in the second stage. In FO, the 2,4,5-T decay was almost stopped in the second stage, but an appreciable decay remained in the second stage in FOU. The reaction mechanisms of the two-step kinetics by FOU and the differences between the FO and FOU can be summarized as follows. Firstly, the rapid decay stage can be ascribed to the fast radical generation induced by several pathways as discussed before with the instantaneous reaction of Oxone and ferrous ions contributing most to the probe decay. It is rational to assume that [Oxone] is approaching the level of depletion at the end of the first stage. When the Oxone becomes deficient, the photodegradation of 2,4,5-T, due to UV photolysis and the hydroxyl radicals generated via the photo-reduction of $Fe(OH)^{2+}$, dominates the secondary stage, where the probe, Fe(II) and Fe(III) are the predominant species in the system.

Based on the above discussions, it can be seen that the involvement of UV is effective in enhancing the process performance with a faster overall reaction rate. In addition, the introduction of UV also demonstrates an advantage of minimizing the required Fe(II) dosage in comparison with FO process for the similar performance.

3.4. Effect of [Oxone]

The efficiency of the FOU process as a function of initial [Oxone] was evaluated by varying its concentration from 0.0625 to 0.75 mM as shown in Fig. 5a. The 2,4,5-T decay increased from 67.6, 87.4 to 98.6% as [Oxone] increased from 0.0625 to 0.25 mM for a 10-min reaction. At lower concentrations, the increase in [Oxone] would lead to the generation of more oxidizing radicals, thereby resulting in the enhancement of the probe decay. However, upon further increasing the [Oxone] to 0.75 mM, no appreciable increment of 2,4,5-T decay can be observed, which is similar to the overdose of H_2O_2 in photo-Fenton process [29,30]. Several reasons have been raised to elucidate this effect, while the radical self-scavenging effect caused by excessive levels of oxidants is the common one [5,31]. Another reason may be the competitive reaction for the radicals between the parent compound and the intermediates. Therefore, further tests were performed to investigate the evolution of 2,4,5-TCP (the major primary intermediate in terms of 2,4,5-T decay by FOU) at various initial [Oxone] (see Fig. 5b). Generally, 2,4,5-TCP is rapidly formed in the first stage, corresponding to the fast disappearance of 2,4,5-T in the first several minutes (see Fig. 5a). After that, the concentration of 2,4,5-TCP gradually or significantly drops depending on the [Oxone]. As the addition of [Oxone] is ≤0.25 mM, the higher the Oxone dosage, the higher generation of 2,4,5-TCP in the first stage and the lower accumulation of 2,4,5-TCP in the final solution. Obviously, as the supply of Oxone is insufficient, higher initial [Oxone] leads to higher generation of

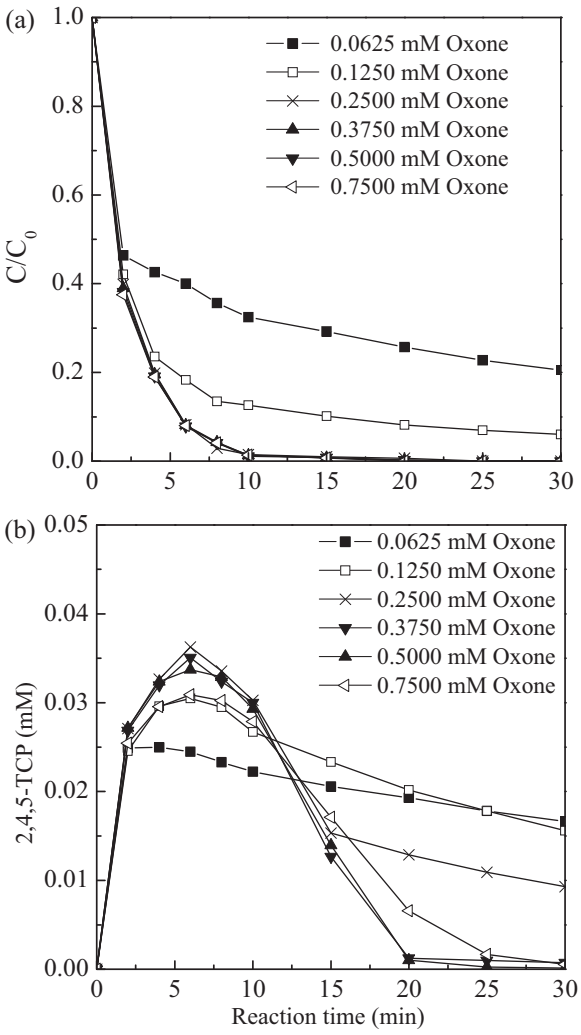

Fig. 5. (a) Photodegradation of 2,4,5-T at different [Oxone] by FOU process. (b) Evolution of 2,4,5-TCP at different [Oxone] by FOU process. *Experimental conditions*: $[2,4,5\text{-T}]_0 = 0.1$ mM, $[Fe(II)]_0 = 0.10$ mM, two 254 nm UV lamps were employed.

powerful radicals, thus resulting in enhanced 2,4,5-T removal and accordingly higher 2,4,5-TCP formation in the solution. After the 2,4,5-TCP reached its maximum concentration at 2–6 min, it gradually decayed, where a linearly decay stage was observed. This suggested that the photo-reduction of Fe(III) and direct photolysis may dominate at this stage after the disappearance of oxidant. As [Oxone] is >0.25 mM, the accumulation of 2,4,5-TCP was lowered in the first 6 min reaction due to faster destructive reaction (in a serial reaction) until its complete disappearance from the 6th to 30th min as compared to the addition of 0.25 mM Oxone. The lower accumulation and complete destruction of 2,4,5-TCP at higher [Oxone] are likely due to the robust generation of both •OH and $SO_4^{\bullet-}$ in the process. The evolution behaviors of the primary intermediate 2,4,5-TCP upon the decay of 2,4,5-T at various [Oxone] suggested that the competition of the probe and the intermediates for oxidizing radicals obviously plays an important role in elucidating the effect of Oxone doses in addition to the commonly recognized radical self-scavenging effect caused by excessive levels of oxidants.

3.5. Variation of 2,4,5-T concentration

To examine the effect of initial probe concentration, tests were carried out by varying [2,4,5-T] from 0.025 to 0.25 mM while keeping other parameters constant as illustrated in Fig. 6a. The

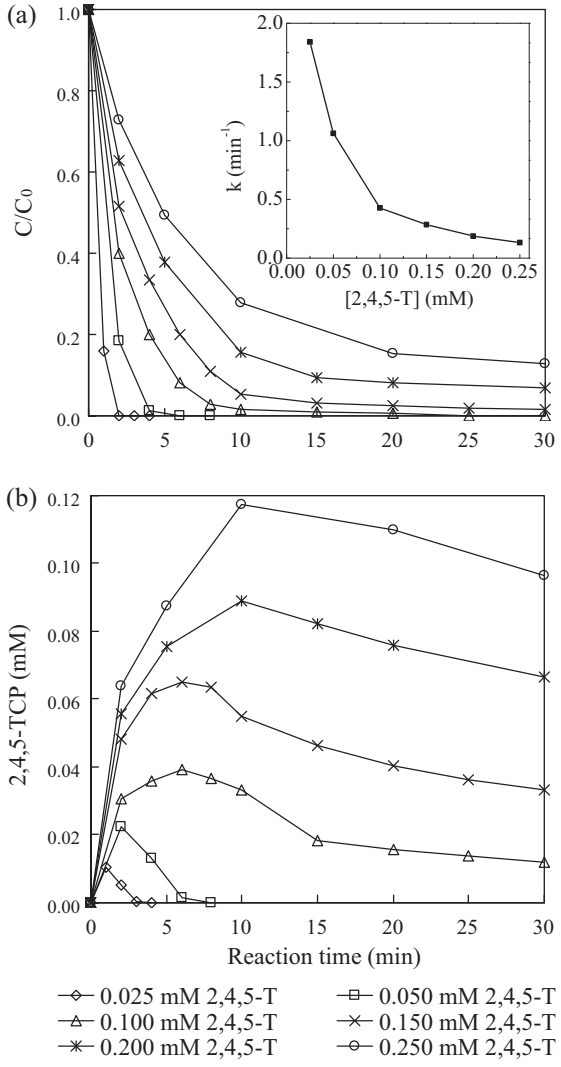

Fig. 6. (a) Photodegradation of 2,4,5-T at different initial concentrations by FOU process. (b) Evolution of 2,4,5-TCP at different [2,4,5-T] by FOU process. *Experimental conditions*: $[Oxone]_0 = 0.25$ mM, $[Fe(II)]_0 = 0.10$ mM, two 254 nm UV lamps were employed.

degradation of 2,4,5-T by FOU process was found to follow pseudo first-order kinetics and the obtained decay rate constant as a function of [2,4,5-T] was depicted in the inset of Fig. 6a. Besides, the corresponding evolution of 2,4,5-TCP at various initial 2,4,5-T concentrations was determined as well (see Fig. 6b). Apparently, the efficiency of probe degradation decreases with increasing initial 2,4,5-T concentration and the decay rate constant was found to decrease from 1.84 to 0.132 min^{-1} as increasing [2,4,5-T] from 0.025 to 0.25 mM. When [2,4,5-T] was ≤0.05 mM, both the 2,4,5-T and 2,4,5-TCP were rapidly removed as can be seen from Fig. 6. This is due to the sufficient supply of Oxone at lower [2,4,5-T]. On the contrary, the degradation of 2,4,5-T at higher initial concentration was significantly inhibited, which might be attributed to the competition reaction of generated degradation intermediates (mainly 2,4,5-TCP, see Fig. 6b) for sulfate and hydroxyl radicals and the depletion of oxidant.

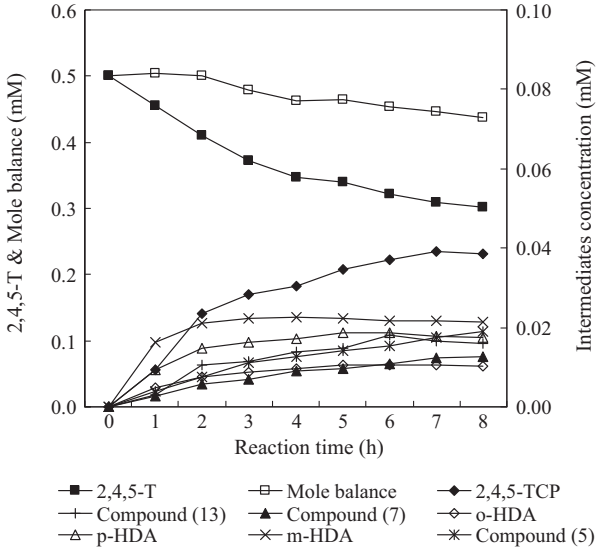

Fig. 7. The evolution profiles of 2,4,5-T and intermediates during the photolysis of 0.5 mM 2,4,5-T under the irradiation of two UV 254 nm lamps.

3.6. Identification of intermediates and decay pathways

In order to identify the degradation intermediates of 2,4,5-T by UV alone, Oxone/UV, and FOU processes with better resolution, initial concentration of the probe was increased to 0.5 mM. The disappearance of 2,4,5-T and the formation and/or destruction of aromatic intermediates were monitored by LC-ESI/MS analysis. Totally, 15 intermediates were identified by the above three processes with the retention time (RT), the molecular weight (MW), and structural formula of the identified intermediates summarized in Table 1. Ten of them have not been previously reported in the literature (compounds **1**–**7**, **10**, **13** and **14**).

3.6.1. UV alone

The LC-ESI/MS analysis revealed that 9 aromatic intermediates were produced during the photo-decay of 2,4,5-T by UV alone (see Table 1). Fig. 7 depicts the trends of 2,4,5-T decay, degradation intermediates, and the mole balance of benzene rings. Compounds **8** and **11** were in trace levels and therefore their formation trends were not shown. Generally, 2,4,5-T decay by direct photolysis is ineffective. The hydrolytic-photolysis of 2,4,5-T through the cleavage of C(1)—O bond (see Eq. (5)) is suggested to be the initial step dominating the 2,4,5-T decay by UV alone as 2,4,5-TCP was observed to be one of the major primary by-products as shown in Fig. 7, where it can be noted that 2,4,5-TCP was formed and gradually accumulated up to 0.0392 mM at 7th hour and declined to 0.0386 mM at the end of the run.

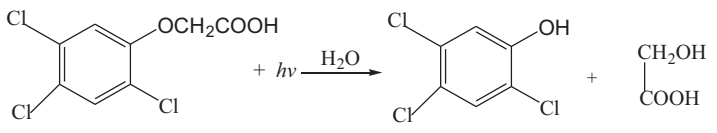

(5)

The dechlorination–hydroxylation is proposed to be the other predominant reaction mechanism, judging from the formation of hydroxyl-dichlorophenoxyacetic acid (HDA). Different isomers corresponding to the possible sites of C—Cl bond cleavage are expected because 2,4,5-T has three chloride at *ortho*, *meta* and *para* locations. They were detected

Table 1
Summary of identified aromatic intermediates determined by LC/ESI-MS upon degradation of 2,4,5-T.

Compound	RT	MW	Structural formula	Detected in		
				UV	UV/Oxone	FOU
2,4,5-T	38.81	255	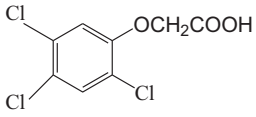	√	√	√
(**1**)	30.51	271.4	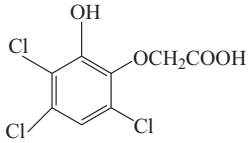		√	√
o-HDA (**2**)	22.82	237	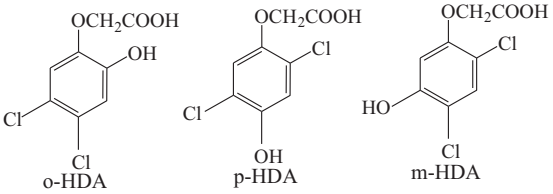 o-HDA p-HDA m-HDA	√	√	√
p-HDA (**3**)	28.51			√	√	
m-HDA (**4**)	29.27			√		
(**5**)	32.09	227.4	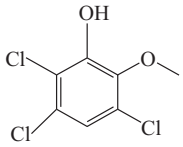	√	√	
2,4-D (**6**)	33.17	221	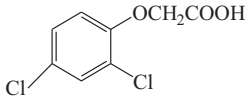			√
(**7**)	16.36	218.5	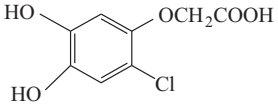	√		
(**8**)	34.16	213.4	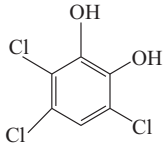	√	√	√
2,4,5-TCP (**9**)	45.02	197.5	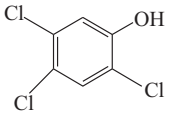	√	√	√
(**10**)	23.07	196	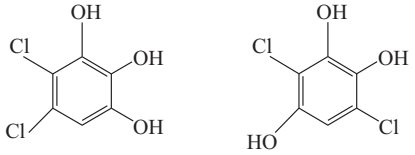		√	√
(**11**)	27.41	179	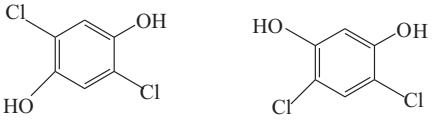	√		√
2,4-DCP (**12**)	39.21	163	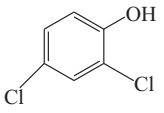			√

Table 1 (*Continued*)

Compound	RT	MW	Structural formula	Detected in		
				UV	UV/Oxone	FOU
(**13**)	15.97	158	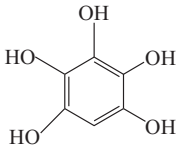	✓		
(**14**)	36.01	144.6	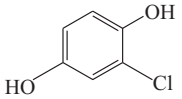 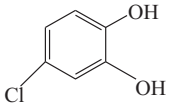			✓
(**15**)	25.92	140	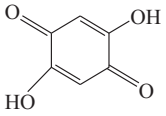			✓

Note: RT is retention time; MW presents molecular weight.

in this study as 2-hydroxy-4,5-dichlorophenoxyacetic acid (o-HDA), 5-hydroxy-2,4-dichlorophenoxyacetic acid (m-HDA), and 4-hydroxy-2,5-dichlorophenoxyacetic acid (p-HDA), respectively. It should be pointed out that the total yield of HDA is much higher than that of 2,4,5-TCP throughout the reaction, suggesting that the decay of 2,4,5-T by UV alone is more easily initiated through the dechlorination–hydroxylation mechanism. Besides, the cleavage of C—Cl bond (339 kJ mol^{-1}) by photon is also thermodynamically preferred due to its lower bonding energy compared with C—O (360 kJ mol^{-1}) and C—H (415 kJ mol^{-1}) bonds. Further dechlorination–hydroxylation of m-HDA and p-HDA leads to the production of secondary intermediate of compound **7**.

Electrophilic aromatic substitution that introduces the hydroxyl group to the benzene ring of 2,4,5-T and electron transfer followed by the loss of CO_2 are believed to be the possible mechanisms leading to the formation of compound **5**. Judging from the low yield of compound **5**, these mechanisms play a minor role. Compound **8** was likely ascribed to the hydroxylation of the benzene ring of 2,4,5-TCP, while compound **8** may undergo dechlorination–hydroxylation giving compound **13** as the tertiary byproduct. Another parallel decay pathway of 2,4,5-TCP is through the further dechlorination–hydroxylation mechanism, justified by the formation of trace compound **11** (2,5-dichlorohydroquinone or 4-6-dichlororesorcinol). It is believed that prolonged irradiation will further degrade these intermediates, leading to the ring-opening with the generation of simpler organics.

3.6.2. Oxone/UV process

Only 7 intermediates (see Table 1) were identified during the Oxone/UV process, probably because some of the daughter compounds were rapidly oxidized by $SO_4^{\bullet-}$ and $^{\bullet}OH$ and became undetectable. The decay of 2,4,5-T and the evolution of the aromatic intermediates are depicted in Fig. 8. Compounds **1** and **8** were not shown due to their trace level. It can be seen that the introduction of Oxone into the UV system significantly promoted the probe decay with over 92% being transformed and over 89% of benzene ring being opened within 180 min. Similar to the UV alone process, 2,4,5-TCP was also identified as the predominant primary intermediate, however, its yield is much higher in Oxone/UV process than that of UV alone as can be seen by comparing Figs. 7 and 8. From Fig. 8, a bell-shape 2,4,5-TCP formation/decay was observed with a peak concentration of 0.192 mM at 60 min, while the accumulation of other intermediates was generally low. The generation of $SO_4^{\bullet-}$ and $^{\bullet}OH$ by the Oxone/UV process clearly contributes to the rapid transformation of 2,4,5-T and its intermediates.

The reaction mechanisms for the decay of 2,4,5-T by Oxone/UV process are therefore proposed as follows: the initial cleavage of the lateral chain via the C(1)—O bond of 2,4,5-T (upon the attacks by $SO_4^{\bullet-}$ and $^{\bullet}OH$) generates 2,4,5-TCP by losing the glycolic acid, which is the dominant mechanism judging from the high yield of 2,4,5-TCP. The mass spectrum of the peak at RT of 30.51 with a m/z of 270 ($[M-H]^-$) denoted as compound **1** was detected in a trace level corresponding to the hydrogen abstraction and followed by monohydroxylation of the aromatic ring on 2,4,5-T. The chemical structure of compound **1** is speculated through the examination of electronic properties of the 2,4,5-T molecule. The $-OCH_2CHOOH$ group in 2,4,5-T with electron-donating character would increase the electron density at the *ortho*- and *para*-positions, while the inductive electron-withdrawing properties of the chlorine atoms significantly reduced the electron density of the adjacent carbon atom. This synthetic effects will render the C(6)-position at the benzene ring with relatively high π-electron density than that of *meta*-position. Thus, the C(6)-position will be more amenable to the electrophilic attack by $SO_4^{\bullet-}$ and $^{\bullet}OH$ as both of them are electrophilic and tend to attack the carbon atoms with higher electron

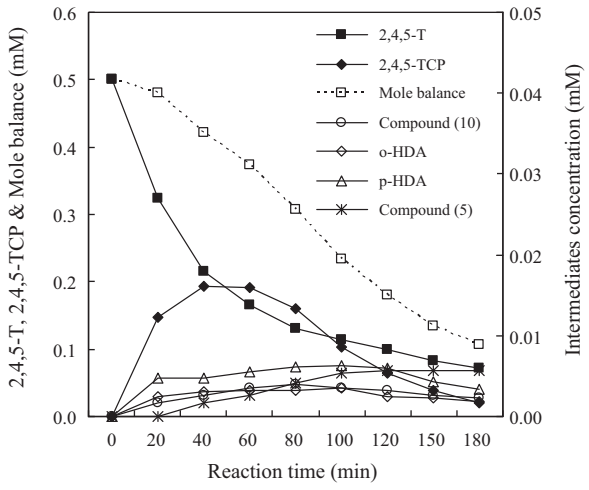

Fig. 8. The evolution profiles of 2,4,5-T and intermediates for the photodegradation of 2,4,5-T by the Oxone/UV process. *Experimental conditions*: $[2,4,5\text{-T}]_0 = 0.5$ mM, $[\text{Oxone}]_0 = 2.5$ mM, two 254 nm UV lamps were employed.

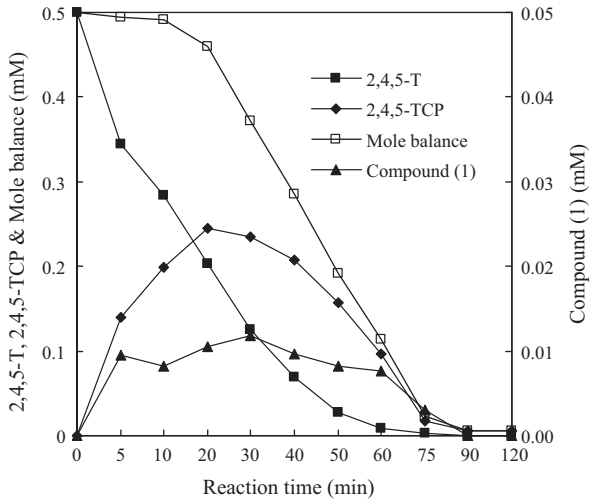

Fig. 9. The evolution profiles of 2,4,5-T and intermediates for the photodegradation of 2,4,5-T by the FOU process. *Experimental conditions*: $[2,4,5\text{-T}]_0 = 0.5$ mM, $[Fe^{2+}]_0 = 0.50$ mM, $[Oxone]_0 = 2.5$ mM, two 254 nm UV lamps were employed.

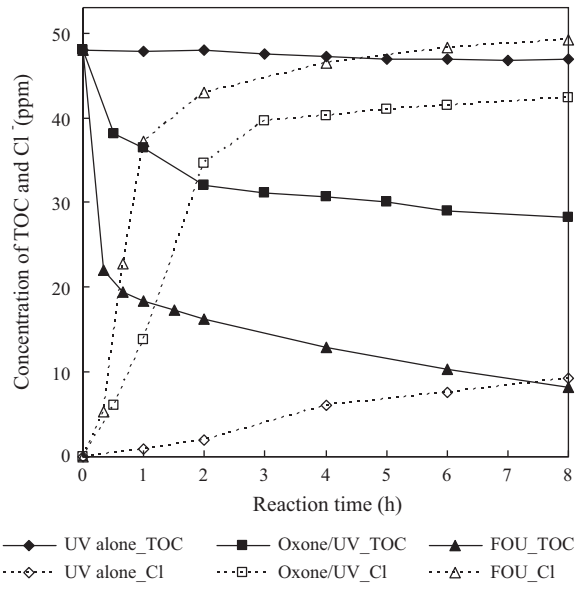

Fig. 10. Time-course of the concentration of TOC, Cl^- for the degradation of 2,4,5-T by UV alone, Oxone/UV and FOU processes.

density. Apart from the electronic influence, the electrophilic addition on the *meta*-position is also disfavored by steric hindrance.

Two HDA isomers were detected resulting from the substitution of chlorine by OH group upon the radical attacks, during which two possible mechanisms may occur: (1) $^{\bullet}OH$ may replace the chlorine atom of 2,4,5-T through attacking the electron-rich positions, and (2) $SO_4^{\bullet-}$ may react via addition to the ring forming in an unstable state and then give sulfate ion as leaving group upon the transfer of an electron and followed by the breaking of C—Cl bond and hydrolysis. It is suggested that the two isomers detected are p-HDA and o-HDA, as the *para*- and *ortho*-positions hold higher electron density than the C(5) position, while *ortho*-position is subjected to more steric hindrance than the *para*-position, rendering the electrophilic attack by hydroxyl and sulfate radicals at the *ortho*-position less favorable compared to the *para*-position, which results in a ratio of 1.81:1 as shown in Fig. 8.

Compound **5** was also detected. The formation mechanism was similar to the UV alone process; except that it is more likely initiated by radical attack in the Oxone/UV process. The subsequent H-abstraction followed by C(6)-hydroxylation of 2,4,5-TCP leads to compound **8** as the secondary intermediate. It may also be formed by the addition of hydroxyl group of compound **1** via the loss of —OCH_2CHOOH group. Further parallel attack of hydroxyl and sulfate radicals on the compound **8** yields the compound **10** with dechlorination. Other further oxidative intermediates were not detectable, probably resulting from the intensified radical supply that destroyed the buildup of these derivatives in the process.

3.6.3. FOU process

In the FOU process, 10 intermediates were identified. However, most of them rapidly disappeared and did not accumulate in the solution. Therefore, their evolution trends cannot be established. Fig. 9 presents the profiles of 2,4,5-T and the major intermediates. The FOU process yielded a more rapid and complete removal of 2,4,5-T giving no trace of any aromatics at the end of the reaction.

The intermediates detected were similar to the Oxone/UV process except that four additional by-products were identified, while compounds **2** and **5** were not observed in the FOU process. The trace compounds **6** (2,4-D) and **12** (2,4-DCP) may originate from the dechlorination of 2,4,5-T and 2,4,5-TCP, respectively. Compound **12** may also be generated from the homolysis of C(1)—O bond on the benzene ring of compound **6** upon radical attack, which is the predominant decay pathway of 2,4-D by $^{\bullet}OH$ attack as reported by Kwan and Chu [32]. Subsequent attack of $SO_4^{\bullet-}$ and $^{\bullet}OH$ on the *ortho*- or *para*-positions may replace the chlorine atom of compound **12** yielding compound **14** (chlorohydroquinone or 4-chlorocatechol) as the tertiary intermediate. Compound **11** is believed to come from the further attack of $SO_4^{\bullet-}$ and $^{\bullet}OH$ on the C(4)- or C(5)-positions of 2,4,5-TCP with the addition of hydroxyl group and the release of Cl^- ion, from a previous study [18]. Compound **11** can undergo further dechlorination-hydroxylation and then be rapidly dehydrogenated to compound **15** (2,5-dihydroxy-*p*-benzoquinone). Further oxidation of compound **15** and other secondary and/or tertiary intermediates will lead to ring opening, resulting in the formation of aliphatics (e.g. carboxylic acids). Judging from the mole balance of benzene ring in Fig. 9, 100% of ring-opening was achieved in 90 min by the FOU process, suggesting all aromatic compounds have been broken down into aliphatic acids in this study. These low molecular organic acids can be further degraded and finally be mineralized to CO_2 as the end product.

Based on the aromatic intermediates identified and above discussions, possible pathways of 2,4,5-T decay by UV alone, Oxone/UV, and FOU processes were accordingly proposed and depicted in Scheme 1.

3.7. TOC removal and time-course of Cl^- ions

Mineralization of 2,4,5-T by UV alone, Oxone/UV and FOU processes were quantified by measuring the TOC contents of the solutions with the results summarized in Fig. 10. The mineralization of 2,4,5-T by UV alone was insignificant, where only 1% of TOC is reduced. In contrast, the Oxone/UV and FOU processes remove 41% and 83% TOC in 8 h, respectively. From Fig. 10, TOC removal by radicals was fast initially and then slowed down at the later stage, which may be attributed to the following reasons: (1) although the mole balance reduction was around 90% in 180 min and 100% in 90 min for the Oxone/UV and FOU, respectively, the aliphatics (e.g. carboxylic acids) formed by the ring-opening reaction of aromatics are more resistant toward further mineralization as reported by previous study [33]; (2) $SO_4^{\bullet-}$ and $^{\bullet}OH$ productions were slowed down duo to the depletion of oxidant along the reaction time. Nevertheless, complete mineralization of 2,4,5-T by the FOU process is possible with sufficient supply of oxidant.

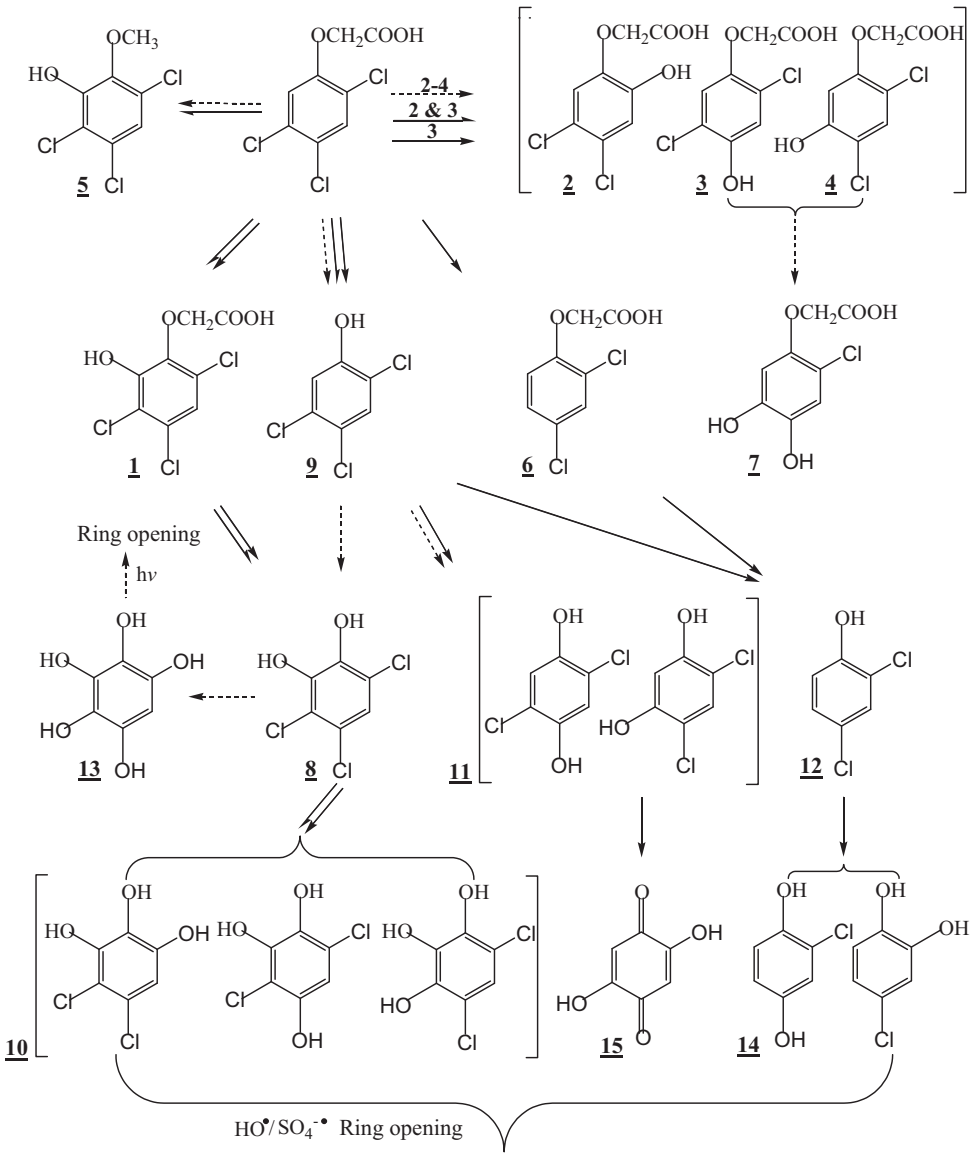

Scheme 1. Proposed decay pathways of 2,4,5-T by UV alone (dotted line), Oxone/UV (solid line with single arrow) and FOU (solid line with double arrow) processes.

The mineralization of 2,4,5-T is expected to be accompanied by the release of chloride ion. This was justified by monitoring [Cl^-] as illustrated in Fig. 10. Similarly, under UV irradiation, [Cl^-] linearly increases at a very slow rate, where ~9.3 ppm of Cl^- was detected at the end of the reaction (8 h). For both of Oxone/UV and FOU processes, the formation of Cl^- was rapid in the first 2 h, corresponding to the fast transformation of 2,4,5-T and the primary intermediate 2,4,5-TCP (see Figs. 8 and 9). The accumulation leveled off at much slower rates afterward, and finally reached 42.3 and 49.2 ppm in 8 h, corresponding to 79.6% and 92.6% of the initial Cl in 2,4,5-T, respectively. The observation of fast initial formation of chloride ions and leveling off at later stage exactly matches the trend of TOC reduction, suggesting the persistence of carboxylic acids or other aliphatics containing chlorine atom toward further mineralization.

4. Conclusions

This study investigated the photodegradation of 2,4,5-T in aqueous solution by Fe(II)-mediated activation of Oxone process with UV irradiation. Comparative experiments between the FO and the FOU process were conducted to elucidate the role of UV light. It was found that the involvement of UV light can significantly accelerate the FO process due to different mechanisms including: direct UV photolysis, radical oxidation by $SO_4^{\bullet-}$ and $^\bullet$OH generated via homolytic cleavage of HSO_5^- upon UV irradiation, radical oxidation by $SO_4^{\bullet-}$ generated by Fe(II)-mediated decomposition of Oxone, accelerated regeneration of Fe(II), and additional production of $^\bullet$OH radicals via photo-reduction of Fe(III)-complexes. 2,4,5-TCP and glycolic acid have been identified as the primary intermediate upon the decay of 2,4,5-T. The accumulation and disappearance of 2,4,5-TCP in terms of 2,4,5-T under various Oxone concentrations demonstrated that the competitive reaction between the parent and daughter compounds for oxidizing radicals plays an important role in explaining the effect of Oxone doses in addition to the commonly recognized radical self-scavenging effect caused by excessive levels of oxidants.

Furthermore, a comparative study upon 2,4,5-T transformation by the sole-UV, Oxone/UV, and FOU processes were conducted. LC-ESI/MS analysis was employed to identify the aromatic intermediates, based on which different decay mechanisms were proposed

and compared. Total 15 aromatic intermediates were identified by these processes, 10 of which have not been previously reported in the literature. Additionally, mineralization in terms of TOC reduction and the release of chloride ions by these three processes have also been comparatively elucidated. It was found that the proposed FOU process demonstrates the best removal (100% in 90 min) of the parent and daughter compounds examined with an outstanding mineralization performance (>83% in 8 h) in comparison with the other two processes.

Acknowledgement

The work described in this paper was fully supported by a grant from the University Research Fund (RPS6) of the Hong Kong Polytechnic University.

References

[1] E.A. Betterton, M.R. Hoffmann, Environmental Science and Technology 24 (1990) 1819–1824.
[2] G.P. Anipsitakis, D.D. Dionysiou, Environmental Science and Technology 37 (2003) 4790–4797.
[3] Y. Cimen, H. Turk, Applied Catalysis A-General 340 (2008) 52–58.
[4] J. Madhavan, P. Maruthamuthu, S. Murugesan, S. Anandan, Applied Catalysis B: Environmental 83 (2008) 8–14.
[5] J. Madhavan, P. Maruthamuthu, S. Murugesan, M. Ashokkumar, Applied Catalysis A-General 368 (2009) 35–39.
[6] A. Rastogi, S.R. Ai-Abed, D.D. Dionysiou, Applied Catalysis B: Environmental 85 (2009) 171–179.
[7] E. Hayon, A. Treinin, J. Wilf, Journal of the American Chemical Society 94 (1972) 47.
[8] H. Gallard, J. De Laat, B. Legube, Water Research 33 (1999) 2929–2936.
[9] E. Brillas, I. Sires, M.A. Oturan, Chemical Reviews 109 (2009) 6570–6631.
[10] J.J. Pignatello, Environmental Science and Technology 26 (1992) 944–951.
[11] P. Neta, V. Madhavan, H. Zemel, R.W. Fessenden, Journal of the American Chemical Society 99 (1977) 163–164.
[12] G.P. Anipsitakis, D.D. Dionysiou, Environmental Science and Technology 38 (2004) 3705–3712.
[13] G.P. Anipsitakis, D.D. Dionysiou, M.A. Gonzalez, Environmental Science and Technology 40 (2006) 1000–1007.
[14] A.J. Chaudhary, M.U. Hassan, S.M. Grimes, Journal of Hazardous Materials 165 (2009) 825–831.
[15] B. Boye, E. Brillas, B. Marselli, P.A. Michaud, C. Comninellis, M.M. Dieng, Bulletin of the Chemical Society of Ethiopia 18 (2004) 205–214.
[16] Guidelines for Drinking-Water Quality, World Health Organization, Geneva, 1996.
[17] M.A. Oturan, J.J. Aaron, N. Oturan, J. Pinson, Pesticide Science 55 (1999) 558–562.
[18] B. Boye, M.M. Dieng, E. Brillas, Electrochimica Acta 48 (2003) 781–790.
[19] E. Brillas, B. Boye, I. Sires, J.A. Garrido, R.M. Rodriguez, C. Arias, P.L. Cabot, C. Comninellis, Electrochimica Acta 49 (2004) 4487–4496.
[20] B. Boye, M.M. Dieng, E. Brillas, Journal of Electroanalytical Chemistry 557 (2003) 135–146.
[21] H.K. Singh, M. Saquib, M.M. Haque, M. Muneer, D.W. Bahnemann, Journal of Molecular Catalysis A: Chemical 264 (2007) 66–72.
[22] Y.F. Rao, W. Chu, Chemical Engineering Journal 158 (2010) 181–187.
[23] W.M. Horspool, Aspects of Organic Photochemistry, Academic Press, New York, 1976.
[24] C.D. Adams, S.J. Randtke, Environmental Science and Technology 26 (1992) 2218–2227.
[25] H. Tamura, K. Goto, YotsuyanT., M. Nagayama, Talanta 21 (1974) 314–318.
[26] G.P. Anipsitakis, D.D. Dionysiou, Applied Catalysis B: Environmental 54 (2004) 155–163.
[27] Y.R. Wang, W. Chu, Journal of Hazardous Materials 186 (2011) 1455–1461.
[28] K.C. Yan, The Degradation of 2,4-4-Dichlorophenoxyacetic Acid Herbicide by Advanced Oxidation System, Dept. of Civil & Structural Engineering, The Hong Kong Polytechnic University, Hong Kong, 2006.
[29] A.G. Trovo, R.F.P. Nogueira, A. Aguera, A.R. Fernandez-Alba, C. Sirtori, S. Malato, Water Research 43 (2009) 3922–3931.
[30] T.M. Elmorsi, Y.M. Riyad, Z.H. Mohamed, H.M.H. Abd El Bary, Journal of Hazardous Materials 174 (2010) 352–358.
[31] S.K. Ling, S.B. Wang, Y.L. Peng, Journal of Hazardous Materials 178 (2010) 385–389.
[32] C.Y. Kwan, W. Chu, Water Research 38 (2004) 4213–4221.
[33] M.A. Oturan, J. Peiroten, P. Chartrin, A.J. Acher, Environmental Science and Technology 34 (2000) 3474–3479.